frontiers in Cellular Neuroscience

TYPE Original Research
PUBLISHED 06 November 2026
DOI 10.3389/fncel.2026.1928157

Check for updates

OPEN ACCESS

EDITED BY
Boldizsár Czéh,
University of Pécs, Hungary

REVIEWED BY
Christina Michalski,
Emory University, United States
Huilin Hong,
Fudan University, China

*CORRESPONDENCE
Michael J. Schmeisser
✉ mschmeisser@uni-mainz.de
Giulia Poggi
✉ poggigiu@uni-mainz.de

RECEIVED 04 July 2026
REVISED 18 October 2026
ACCEPTED 21 October 2026
PUBLISHED 06 November 2026

CITATION
Reuss SG, Wicki S, Schmid S, Hogg DE, Müller MB, Pryce CR, Schmeisser MJ and Poggi G (2026) Subtle microglia and oligodendrocyte precursor cell histological changes across social stress paradigms.
Front. Cell. Neurosci. 20:1928157.
doi: 10.3389/fncel.2026.1928157

COPYRIGHT
© 2026 Reuss, Wicki, Schmid, Hogg, Müller, Pryce, Schmeisser and Poggi. This is an open-access article distributed under the terms of the Creative Commons Attribution License (CC BY). The use, distribution or reproduction in other forums is permitted, provided the original author(s) and the copyright owner(s) are credited and that the original publication in this journal is cited, in accordance with accepted academic practice. No use, distribution or reproduction is permitted which does not comply with these terms.

Subtle microglia and oligodendrocyte precursor cell histological changes across social stress paradigms

Senta G. Reuss[1,2], Sarah Wicki[3,4,5], Sophie Schmid[3], David E. Hogg[3], Marianne B. Müller[1,2], Christopher R. Pryce[3,4,5], Michael J. Schmeisser[6,7]* and Giulia Poggi[1,6]*

[1]Department of Psychiatry and Psychotherapy, University Medical Center of the Johannes Gutenberg-University Mainz, Mainz, Germany, [2]Leibniz Institute for Resilience Research, Mainz, Germany, [3]Preclinical Laboratory for Translational Research into Affective Disorders, University Hospital of Psychiatry and University of Zurich, Zurich, Switzerland, [4]University Research Priority Program (URPP), Adaptive Brain Circuits in Development and Learning (AdaBD), University of Zurich, Zurich, Switzerland, [5]Neuroscience Center Zurich, University of Zurich and ETH Zurich, Zurich, Switzerland, [6]Institute of Anatomy, University Medical Center of the Johannes Gutenberg-University Mainz, Mainz, Germany, [7]Focus Program Translational Neurosciences, University Medical Center of the Johannes Gutenberg-University Mainz, Mainz, Germany

Social stress is a key risk factor for disorders of increased aversion responsiveness, and changes in cortico-limbic oligodendrocyte lineage and myelination may contribute to this pathological process. In adult male mice, we demonstrated previously that social stress-induced aversion hyper-responsiveness co-occurs with altered oligodendrocyte proliferation-maturation dynamics and myelin content. Overall, however, findings on these inter-relationships are inconsistent across studies using various stress paradigms, suggesting that there is not a simple relationship between social stress and the extent and direction (i.e., loss vs. gain) of changes in the oligodendrocyte lineage and myelin. Under physiological conditions, the immune cells of the CNS, microglia, monitor the CNS microenvironment and contribute to oligodendrocyte lineage and myelin homeostasis. Also, recent reports suggest that microglia state might influence oligodendrocyte lineage changes in response to certain social stress paradigms. Here, we begin to address the hypothesis that social stress induced changes in microglia and oligodendrocyte lineage are inter-related in mice. We employed histological and semi-automated image analyses to characterize a subset of microglia and OPC histological properties in medial prefrontal cortex (mPFC) and basal amygdala (BA) following aversive social experiences, including chronic social stress (CSS), CSS followed by aversion learning (excessive aversive stimulation), and social isolation (as the absence of sociopositive stimulation). Specifically, we assessed: (1) the density and proliferation rate of microglia and OPCs; (2) the spatial relationship between microglia and OPCs; and (3) microglia morphological complexity as a proxy for their activity/state. The preliminary integrative histological evidence is for subtle stress paradigm-associated alterations in microglia- and OPC-related features, and limited correlative histological associations between these cell populations.

KEYWORDS
aversion learning, basal amygdala, microglia, mPFC, oligodendrocyte precursor cells, social stress

1 Introduction

In their natural environments, organisms are exposed constantly to a myriad of environmental challenges that shape physiology and behaviour, resulting in dynamic homeostasis and adaptation through a finely-tuned feedback loop (de Kloet et al., 2005). However, when challenges are extreme and/or prolonged, as is often the case in modern human societies, this delicate equilibrium can be perturbed, with detrimental consequences on mental and physical health (de Kloet et al., 2005). Among these challenges, adverse social experiences represent one of the most prevalent and potent forms of *stress* (Wood and Bhatnagar, 2015). Social stress—including isolation, bullying, bereavement, and psychological abuse—is a key trigger for disorders of increased aversion responsiveness, such as major depression and anxiety disorders. These disorders are associated with functional changes in the anterior cingulate cortex (ACC)-amygdala bidirectional pathway (medial prefrontal cortex (mPFC)-amygdala in rodents) (Poggi et al., 2024), which is integral to the neural circuitry of socio-emotional processing (Murphy et al., 2016; García-Cabezas and Barbas, 2017; Allsop et al., 2018; d'Arbeloff et al., 2018). Clinical and preclinical studies suggest that these alterations might involve within- and between-regional changes in the oligodendrocyte lineage and myelination (Poggi et al., 2024). Specifically, it has been postulated that aversive social experience can alter myelin/oligodendrocyte-specific transcript and protein levels, oligodendrocyte proliferation-maturation dynamics, and myelin content (Laine et al., 2018; Bonnefil et al., 2019; Cathomas et al., 2019; Pan et al., 2020; Kokkosis et al., 2022; Poggi et al., 2022; Koskinen et al., 2023). However, consensus on the specific underlying cellular mechanisms and on the direction of such changes has not been reached.

Studies with juvenile or adult rodent social-isolation paradigms have shown, rather equally, that social deprivation does (Liu et al., 2012; Makinodan et al., 2012; Zhang et al., 2022) or does not (Lander et al., 2017), lead to changes in myelin-related transcripts, the oligodendrocyte lineage and myelin content in the mPFC. Also, multiple studies based on the resident-intruder paradigm have investigated the consequences of chronic psychosocial stress on behaviour and brain functions (e.g., Wallace et al., 2009; Golden et al., 2011; Sigrist et al., 2024; Poggi et al., 2025). In these paradigms, the experimental mouse is located in the home cage of a larger, aggressive and territorial mouse (typically of the CD-1 strain) for a short period of direct contact—which includes fighting and physical defeat—followed by 24 h of distal stressor exposure. The duration of the daily physical defeat, as well as the total length of the protocol varies across studies, ranging from 30 s to 10 min for the daily physical defeat and from 10 to 21 days for the duration of the overall protocol (Díez-Solinska et al., 2024). These stress protocols induce specific anxiety- and depression-relevant behavioural alterations, including social deficits, aversion biases and reduced reward responsiveness, but have yielded conflicting results with respect to myelin and oligodendrocytes dynamics (Poggi et al., 2024). For instance, the paradigms chronic social defeat (CSD, (Golden et al., 2011)) and repeated social defeat stress (RSDS, (Kokkosis et al., 2022, 2024; Madeira et al., 2025))—which allow for stratification into susceptible and resilient mice—lead to reduced myelin content in the mPFC (Lehmann et al., 2017; Bonnefil et al., 2019; Kokkosis et al., 2022). Furthermore, focal demyelination in mPFC reproduces the social avoidance phenotype typically observed following CSD (Bonnefil et al., 2019). In contrast, chronic social stress (CSS), which increases aversion responsiveness in Pavlovian aversion learning and memory (PALM, (Azzinnari et al., 2014; Sigrist et al., 2024; Poggi et al., 2025)) and decreases reward responsiveness in operant learning and memory (Bergamini et al., 2016; Madur et al., 2023), leads to increased myelin content in the mPFC (Poggi et al., 2022). Whether alterations in oligodendrocyte lineage and myelin content per se, irrespective of the direction, might be causally relevant to stress-related brain-behavioural changes remains an open question.

Microglia are the immune cells of the central nervous system (CNS). Under physiological conditions, microglia monitor the CNS microenvironment continuously and play a key role in maintaining oligodendrocyte lineage and myelin homeostasis (Nicholas et al., 2001; Miron et al., 2013; Hagemeyer et al., 2017; Santos and Fields, 2021; Sherafat et al., 2021; McNamara et al., 2023). Under certain conditions, the density of the oligodendrocyte lineage correlates with microglia density, and it has been shown that microglia can recruit oligodendrocyte precursor cells (OPCs) to the area where (re)myelination is required, influence OPC differentiation, and shape myelin plasticity under both physiological and pathological conditions (Wolswijk, 2002; Patani et al., 2007; Kalafatakis and Karagogeos, 2021). Notably, evidence indicates that the rodent adult social stressors CSD and RSDS are associated with high inflammatory response and pronounced microglia reactivity (Lehmann et al., 2016, 2018, 2019; Kokkosis et al., 2022, 2024; Madeira et al., 2025), specifically in stress-susceptible mice, while CSS is associated with a mild inflammatory response (Azzinnari et al., 2014; Grandjean et al., 2016; Cathomas et al., 2019). Furthermore, it has been reported that social isolation leads to age- and brain region-specific changes in microglia reactivity (Ferrara et al., 2022) and social behaviour is altered following microglia depletion (Zhan et al., 2014; Ferrara et al., 2022). This raises the possibility that distinct microglial activation patterns may underlie the divergent effects of different social stressors on the oligodendrocyte lineage and myelination.

Here, we tested the hypotheses that different social stress paradigms—carried out also at different stages of life—vary in their effects on microglia properties and on microglia–OPC interdependence. Firstly, we employed publicly available gene expression dataset and performed an exploratory evaluation of microglia transcriptional patterns in the mPFC of mice that had undergone the CSD paradigm, associated with demyelination, and of mice that had undergone the CSS paradigm, associated with myelin increase. We then employed histological and semi-automated image analyses to characterise microglial density, proliferation, morphology (as a proxy for microglia state), and spatial relationships with OPCs after CSS, CSS followed by aversive learning experiences, and social isolation. Our findings provide preliminary evidence for subtle stress paradigm-associated alterations in microglial- and OPC-related features, with no clear histological evidence for associations between these two cell populations.

2 Materials and methods

2.1 *In vivo*

2.1.1 Animal and maintenance

The experiments were conducted with male C57BL/6 J mice, bred in-house. After weaning they were maintained in littermate

pairs (if not stated otherwise, due to experimental procedure) in individually ventilated type 2 L cages at 20–22 °C and 50–60% humidity under a reversed 12:12-h light–dark cycle. Each of the reported experimental procedures was conducted during the dark phase. Food (Complete pellet Provimi, Kliba Ltd., Kaiseraugst, Switzerland) and water were available ad libitum. Resident mice for the CSS protocol were ex-breeder males of the CD-1 strain (Janvier Labs, Saint-Berthevin, France) aged 8 months and caged singly. All experiments were conducted under animal experimental license issued by the Veterinary Office of Canton Zurich (licenses: ZH-149/2015, ZH-155/2018 ZH093/2019, ZH-174/2021, and ZH-038/2022).

2.1.2 Pavlovian aversion learning test

Pavlovian aversion learning (PAL) involves the acquisition of an association between an initially neutral environment (context) and stimulus (conditioned stimulus, CS) and an innate aversive stimulus (unconditioned stimulus, US) (Poggi et al., 2025). The testing was conducted using an automated system fitted with infrared-beam detection of (no-)movement (Multi-Conditioning System, TSE Systems GmbH, Bad Homburg, Germany) (Azzinnari et al., 2014; Poggi et al., 2025). A novel auditory tone of 6.5 kHz and 85 dB was employed as CS, while a 2 s x 0.25 mA electro-footshock was employed as US. The PAL paradigm comprised 2 stages. One stage was conducted per day, each within the same context. The percentage time spent in freezing behaviour, i.e., a state of making no detectable movement during at least 1 s, was used as the quantitative conditioned response. *Stage 1, habituation*. The mouse was placed on the grid floor in the context for 15 min. Freezing behaviour was recorded continuously. This habituation stage was performed both prior to and after the 15-day CSS protocol. The pre-CSS protocol freezing data were used to counterbalance allocation of littermate pairs to the CON and CSS groups. The post-CSS habituation freezing scores were used to measure aversion responsiveness toward a neutral environment. *Stage 2, tone-footshock (CS-US) conditioning*. The mouse was placed on the grid floor in the same context and, after 5-min adaptation, exposed to 6 CS-US trials with an intertrial interval (ITI) of 120 s. Each CS-US trial consisted of a 20-s auditory CS and a 2-s electro-footshock US delivered on seconds 19–20 of the CS. Percent time freezing was measured during the six CSs (sec 1-18). For the analysis, the trials were binned into CS-US blocks 1–2, 3–4, 5–6.

2.1.3 Chronic social stress: experimental design

Three experiments were performed with young adult male C57BL/6 J mice. In ***Experiment 1***, 10-week-old mice were exposed to either CSS (CSS, $n = 14$) or control handling (CON, $n = 12$) and received 5-ethynyl-2′-deoxyuridine (EdU; Cat. No. E10187, ThermoFisher Scientific) via the drinking water throughout. One-half of the mice of each group was transcardially perfused 24 h after the termination of the CSS protocol (day 16), and the other half after an additional 15 days (day 31). The brains were collected for histological assessment. A detailed description of the procedure is available elsewhere (Poggi et al., 2022). In *Experiment 2*, 10-week-old mice were exposed to either CSS (CSS, $n = 5$) or control handling (CON, $n = 5$) for 15 days and transcardially perfused 24 h after the termination of the protocol (day 16). In *Experiment 3*, 10-week-old mice were exposed to either CSS (CSS, $n = 8$) or control handling (CON, $n = 8$) for 15 days, exposed to PAL and transcardially perfused 90 min after the CS-US conditioning phase of the PAL protocol (day 17).

2.1.3.1 Chronic social stress protocol

The CSS procedure was performed as previously described (Azzinnari et al., 2014; Sigrist et al., 2024). Briefly, the cages of ex-breeder CD-1 aggressive male mice were divided into two equal compartments by a transparent, perforated plexiglass divider. For 15 consecutive days, each C57BL/6 J mouse assigned to the CSS group was located within the same compartment as an unfamiliar CD-1 resident mouse. The mice were maintained together for a maximum of 60s fight/attack or 10 min, whichever occurred sooner. Thereafter the C57BL/6 J mouse remained in the compartment of the cage where the attack took place, and the CD-1 mouse was transferred to the other compartment. Distal exposure between the two mice occurred for the following 24 h, after which C57BL/6 J mice were rotated between CD-1 cages. Critically, to prevent bite wounds, typically observed in the conventional chronic social defeat (CSD) protocol (Golden et al., 2011) and which could initiate a confounding inflammatory response (Süß et al., 2020), the lower incisors of the CD-1 mice were trimmed every third day (Azzinnari et al., 2014; Fuertig et al., 2016). CON mice remained in littermate pairs and were handled and weighed on each of the 15 days. After the termination of the CSS protocol and before perfusion, CSS mice were maintained in distal exposure to the same CD-1 mice, and no further attack session was carried out. For the mice that were sacrificed on day 31 (CSS Experiment 1), the compartment allocation within the same cage was swapped daily (Poggi et al., 2022). This ensured constant direct exposure to the stressful sensory stimuli of CD-1 mouse bedding.

2.1.4 Juvenile social isolation: experimental design

Briefly, C57BL6/J mice were weaned between postnatal day (P)20 and P22 (mean P21) and caged with 1, or occasionally 2, male littermates, and were allocated to either social isolation (SI, $n = 8$) or social rearing (SR, $n = 8$) groups. From week 5 to week 9, the mice were left undisturbed under their assigned housing conditions, except for standard daily checks and cage changes. In week 9, the mice were sacrificed. For further details, see (Wicki et al., 2026).

2.2 Ex-vivo

2.2.1 Tissue preparation

At the end of each experiment, mice were deeply anaesthetized with sodium pentobarbital (150 mg/kg) injected intraperitoneally. The tissue preparation of each experiment was tailored according to its main histological aim. *CSS - Experiment 1*. Mice were transcardially perfused with 15 mL of 1x PBS (pH 7.4) at RT followed by 50 mL of ice-cold 4% paraformaldehyde (PFA) in 0.1 M sodium phosphate buffer (pH 7.4). Perfusion rate was maintained at 20 mL/min. The brains were post-fixed for 2 h in 4% PFA at 4 °C, and dehydrated in 30% (w/v) sucrose in 1x PBS for 48 h at 4 °C. The brains were then embedded in a cryoprotectant medium (Tissue-Tek, O. C. T., Cat. No. 4583, Sakura Finetek Europe) and stored at -80 °C until further

processing (Poggi et al., 2022). *CSS - Experiment 2, CSS - Experiment 3.* Mice were transcardially perfused with 15 mL of 1x PBS (pH 7.4) at RT followed by 50 mL of ice-cold 4% PFA in 0.1 M sodium phosphate buffer (pH 7.4). Perfusion rate was maintained at 20 mL/min. The brains were post-fixed for 4 h in 4% PFA at 4 °C, and dehydrated in 30% (w/v) sucrose in 1x PBS for 48 h at 4 °C. The brains were then embedded in a cryoprotectant medium (Tissue-Tek, O. C. T., Cat. No. 4583, Sakura Finetek Europe) and stored at -80 °C until further processing. *Juvenile social isolation experiment.* Mice were perfused with 10 mL of 1x PBS (pH 7.4, RT) followed by 30 mL of ice-cold 4% PFA in 0.1 M sodium phosphate buffer (pH 7.4). Perfusion rate was maintained at 10 mL/min. The brains were post-fixed in 4% PFA for 2 h, at 4 °C. For subsequent cryoprotection, the brains went through a ramping scale of sucrose solutions in 1x PBS: 10%, 15%, 30%, each for 24 h at 4 °C. The brains were then embedded in cryoprotective medium (Tissue-TEK O. C. T. Compound, Sakura Finetek) in a cryomold and stored at -80 °C until further processing (Wicki et al., 2026).

2.2.2 Sectioning and storage

Coronal brain sections including the mPFC (bregma: ~ + 2.0 mm) and the BA (bregma: ~ -1.80 mm) were cut at 40 µm using either a freezing microtome (Histocom AG, Switzerland) or a cryostat (Leica). Sections were collected and briefly rinsed in 1x PBS (pH 7.4, RT) and transferred into a 96-well plate filled with tissue collection solution (250 mL glycerine, 300 mL ethylene glycol, 250 mL 0.2 M PO_4, 250 mL dH_2O). The 96-well plates were stored at -20 °C until immunofluorescence staining was conducted.

2.2.3 Immunofluorescence staining

CSS - Experiment 1. The 40 µm coronal cryopreserved sections were washed for 1 h (3 × 20 min) to remove any residual cryoprotective medium. EdU labelling was conducted using the Click-iT™ EdU Cell Proliferation Kit for Imaging (C10337 or C10339, ThermoFisher Scientific) according to the manufacturer's instructions. Sections were blocked with 10% donkey serum in 0.5% (v/v) Triton X-100 in PBS for 1 h at RT. They were then incubated with the primary antibodies diluted in 3% donkey serum in 0.5% Triton X in PBS for approximately 18 h at 4 °C. The employed antibodies were: rabbit polyclonal anti-NG2 (1:250; AB5320, Merck-Millipore) for OPCs, rabbit anti-Iba1 (1:500; 019–19,741, Wako) and rat monoclonal anti-CD68 (1:1000, MCA1957GA, Serotec) for microglia, and rabbit anti-ASPA/Nur7 (1:500; ABN1698, Merck-Millipore) for mature oligodendrocyte. The sections were then incubated with appropriate fluorophore-conjugated secondary antibodies (1:500; Alexa Fluor Secondary Antibodies, Thermofisher) in 3% donkey serum in 0.5% (v/v) Triton X-100 for 2 h at RT. The sections were then mounted on SuperFrost slides (10,149,870, ThermoFisher) and cell nuclei were stained directly by addition of DAPI Fluoroshield Mounting Medium (F6057, Merck). Due to the host species of the primary antibodies, not all stainings could be combined on the same sections, and they were therefore performed separately on adjacent sections (Poggi et al., 2022).

CSS - Experiment 2, CSS - Experiment 3, Juvenile social isolation experiment. The 40 µm coronal cryopreserved sections were subjected to 3 × 20 min washes in PBS (18912-014, Gibco). Thereafter, the sections were incubated in 0.5% Triton X-100 (3051.3, Roth) in 1X PBS for 1.5 h at RT and blocked in 5% donkey and 5% goat serum in 0.5% Triton X-100 in 1X PBS for 1 h at RT. The sections were then incubated for approximately 18 h at 4 °C with three primary antibodies diluted in 0.5% Triton X-100 in 1X PBS with 1.5% each of donkey serum and goat serum. The employed primary antibodies were rabbit anti-Pdgfr**α** (1:200, 3174S, Cell Signaling Technology) for OPCs, rat anti-Ki-67 (1:200, 14-5698-82, eBiosciences) for proliferative cells, and guinea pig anti-Iba1 (1:500, HS-234308, Synaptic Systems) for microglia. Importantly, as all non-vascular $NG2^+$ cells in the mouse co-express Pdgfr**α** (Rivers et al., 2008), it is reasonable to assume that both markers identify substantially overlapping OPC populations. This is further supported by a qualitative comparison showing that the overall density of $NG2^+$ cells, with typical OPC morphology, in mPFC and BA of CON mice in the previously published dataset (Poggi et al., 2022) was comparable to the overall density of Pdgfr**α**$^+$ cells in the relevant control mice of each study included in this manuscript (i.e., in the order of 400 cells/mm2 on average). Thus, although differences in antibody specificity, and tissue processing preclude assuming a complete equivalence between the two markers, they show sufficient analogy to allow qualitative comparison between experiments. Also, as we observed that all the IBA1 + cells co-expressed CD68 in Experiment 1, and because Ki-67 could not be co-stained with CD68 on the same section due to their identical host species, we relied exclusively on anti-IBA1 staining to identify microglia. On the following day, after 3 × 20 min washes in 1X PBS, the sections were incubated with fluorophore-conjugated secondary antibodies (1:500; Alexa Fluor Secondary Antibodies, Thermofisher) in 1.5% donkey serum and 1.5% goat serum in 0.5% Triton X-100 in 1X PBS for 2 h at RT. The sections were then washed 3 × 20 min in 1X PBS, incubated with DAPI solution for cell nuclei staining for 5 min at RT, and additionally washed for 3 × 10 min in 1X PBS. The sections were mounted on Superfrost Plus Adhesion Microscope Slides (10,149,870, ThermoFisher) with Fluoroshield Mounting Medium (F6182-20ML9).

2.2.4 Microscopy and image analysis

CSS - Experiment 1. Micrographs of mPFC and BA were acquired at a confocal laser scanning microscope Leica Sp8, with an HC PL APO CS2 20x NA 0.75 multi-immersion objective in standard mode (Pinhole = 1 AU; pixel size to 0.3342 × 0.3342 μm^2; z-stack interval = 2 µm) (Poggi et al., 2022). *CSS - Experiment 2, CSS - Experiment 3, Juvenile social isolation experiment.* Images of the mPFC and BA were acquired at a light microscope (AxioObserver with Apotome 3, Zeiss) with a 20x non-immersion objective (NA: 0.55, working distance: 26 mm). Voxel size was set to 0.293 × 0.293 × 0.49 μm^3, with 14 BitsPerPixel. For quantification of cell contact and colocalization (as proxy of phagocytosis-relevant events), confocal micrographs were acquired with a HC PL APO CS2 63x/1.40 oil objective; pinhole was set to 1 AU, the image format to 1,024 × 1,024 pixels, and the pixel size to 86 × 86 × 150 nm^3. Image analysis and quantification were performed with semi-automated workflows on Imaris (Oxford Instruments)[1] by two independent experimenters. The following outputs were collected: (1) density of Pdgfr**α**$^+$-, $Iba1^+$-, $KI\text{-}67^+$-cells, (2) length and complexity of $Iba1^+$ cells (Sholl analysis, operationalised as

1 https://imaris.oxinst.com

the number of intersections between microglial processes and concentric spheres spaced at 1-μm radial intervals, centred on the cell body), (3) shortest distance between Pdgfrα^+ and Iba1$^+$ cells (as shortest distance between the centre of the cell bodies), and (4) size and frequency of contacts and co-localisation between Pdgfrα^+ and Iba1$^+$ cells (*surface contact* in case of distance between surfaces = 0; *voxel co-localisation* in case of distance between surfaces <0). Detailed IMARIS pipelines and algorithm settings are available in the supplementary IMARIS WORKFLOWS section.

2.2.5 In-silico

For an exploratory analysis of social stress-induced differences in microglia-relevant pathways that co-occur with divergent changes in myelin and oligodendrocyte lineage, a qualitative comparison was carried out between: (1) a microarray dataset obtained with a CSD versus control protocol that led to mPFC myelin loss [derived from Gemma, GSE84572 - GPL6246 - Affymetrix Mouse Gene 1.0 ST Array, (Lehmann et al., 2017)], and (2) a bulk-RNA sequencing dataset (Illumina HiSeq2000 Sequencer) obtained with a CSS versus control protocol and subjected to differential gene expression and deconvolution analysis (Cathomas et al., 2019), where the CSS protocol is known to lead to increased myelin content in mPFC (Poggi et al., 2022). Using an over-representation analysis (ORA) approach, transcripts that were differentially expressed in stress versus control mice were selected from each of these datasets. These transcripts were then sorted based on the direction of the change (fold-change > 0 and fold-change < 0). Thus 4 separate subsets of data were obtained: (1) Upregulated post-CSD in Lehmann et al. (L↑), (2) Downregulated post-CSD in Lehmann et al. (L↓), (3) Upregulated post-CSS in Cathomas et al. (C↑), (3) Downregulated post-CSS in Cathomas et al. (C↓). Microglia pathway enrichment analysis was performed on each subset via MGEnrichment (Jao and Ciernia, 2021)[2] and the extent of overlapping microglia pathways was estimated via Jaccard overlap index. The observed Jaccard index was tested against random effects with a permutation test (n = 5,000). Given the exploratory purpose of this analysis and the different transcript expression platforms employed for the original analysis of the two datasets (microarray vs. bulk-RNA sequencing), the depth of the current exploratory analysis has been kept at the level of pathways and no specific investigation at single-transcript level has been performed. The list of genes included in the exploratory analysis can be found in the Table 1.

2.3 Statistics

Statistical analyses were conducted with GraphPad Prism software (GraphPad, version 11.0.2). Microglia enrichment analysis and permutation were carried out with MGEnrichmentApp (Jao and Ciernia, 2021; see footnote 1) and AI-supported custom-designed Python scripts. Sample distribution was assessed via Shapiro–Wilk normality test. Correlation was assessed via Pearson's test. Importantly, it should be noted that, given the small sample size in the included experiments, no comparison of correlation coefficients was carried out. The presence (or absence) of correlation was intended exclusively as a descriptive observation of the relationship between histological parameters of OPC and microglia in defined experimental conditions. Additionally, for completeness of the statistical analysis and to account for multiple testing, nominal p-values were additionally subjected to Benjamini–Hochberg false discovery rate (BH-FDR) correction. Analyses were grouped into biologically defined families according to experimental cohort and outcome domain: (1) *cell-density correlations*, (2) *cell density*, (3) *microglia morphology*, and (4) *microglia–OPC proximity/contact*. Of the 14 possible cohort x outcome combinations, only 12 contained actual new analyses and were, therefore, subjected to the indicated correction. Previously published analysis and combinations without new testing were not included. The FDR-adjusted p-values are reported in Supplementary Table 1 as a complementary assessment of the robustness of the nominal statistical observations. Data are shown as mean ± standard deviation (S.D.). Individual data points are also given in the graphs. Statistical significance was set at $p < 0.05$ for all tests. The number of biological replicates (n), specific statistical tests, and their p-values are indicated in the figure legends. A biological replicate in the reported statistical models corresponds to one individual mouse. Specifically, for the assessment of cell density, the mean cell density of each hemisphere per brain regions per mouse was employed; for the assessment of microglia morphology, the mean of the intersections at each defined radius for all the detected cells per brain region per mouse was employed and >100 cells per mouse were included in the analysis; for the assessment of proximity and contact, the mean of the shortest distance or number of contact for all the detected cells per brain region per mouse was employed. Further details are reported in the relevant figure legend.

3 Results

3.1 CSS does not lead to substantial morphological and spatial rearrangements of microglia

Both loss or gain of OPCs, oligodendrocytes, and myelin in brain regions integral to the neural circuitry of aversion processing have been reported for specific stress paradigms and might contribute to the behavioural states induced by these paradigms. Notably, these changes often co-occur with diverse microglia responses, which in turn appear to be dependent on the stress paradigm. Since microglia have been implicated in the regulation of oligodendrocyte lineage functions (Santos and Fields, 2021; McNamara et al., 2023), it is conceivable that chronic social stress paradigms associated with oligodendrocyte lineage and/or myelin loss or gain induce different changes in microglia. An exploratory comparison of publicly available mPFC transcriptomic datasets from studies of CSD [associated with oligodendrocyte and myelin loss (Lehmann et al., 2017)] and CSS [associated with preservation of oligodendrocyte lineage density and myelin increase (Cathomas et al., 2019; Poggi et al., 2022)] revealed limited overlap in microglia-related enriched gene sets (Supplementary Figure S1 and Table 1), suggestive of the possibility that distinct social stress paradigms engage different microglial response.

With the dataset from *Experiment 1* (Supplementary Figure S2A) we already reported that CSS leads to reduced proliferative OPCs in

2 https://ciernialab.shinyapps.io/MGEnrichmentApp/

mPFC and BA and no changes in overall OPCs density or in microglia density and proliferation (Poggi et al., 2022). However, unaltered cell density and proliferation do not exclude the contribution of microglia to oligodendrocyte lineage changes in the processing of aversive experience. In various physiological and pathological instances, known to impact on the oligodendrocyte lineage, a correlation between microglia density and the density of cells of the oligodendrocyte lineage has been observed (Wolswijk, 2002; Patani et al., 2007; Kalafatakis and Karagogeos, 2021). Here, we report that the proliferative OPC density correlated negatively with microglia density in mPFC and BA in CSS mice (Supplementary Figure S2C,E), whereas no significant correlation was detected in CON mice (Supplementary Figures S2B,D). The overall OPC density correlated positively with microglia density in the mPFC in CSS mice (Supplementary Figure S2C). In CON mice this phenomenon was not detected (Supplementary Figures S2B). Notably, such correlations were not observed between microglia and mature OL, in either CON or CSS mice (Supplementary Figures S2B–E).

In a small cohort of brains available from CSS *Experiment 2*, we co-stained the OPC marker Pdgfrα, the microglia markers Iba1 and the end-point proliferation marker Ki-67 on a single coronal section per region of interest. We estimated cell density, microglia complexity (as a proxy for microglia state), and microglia and OPC proximity and contact (*Experiment 2*, Figure 1). Notwithstanding the small sample size, in CSS mice and not CON mice, OPC density increased with microglia density, thereby aligning with the finding in Experiment 1. In contrast to Experiment 1, there was no indication of an association between the density of end-point proliferative OPCs and microglia (Supplementary Figure S3). Microglia morphology was comparable between groups in both mPFC and BA (Figures 1C,F), providing no histological evidence for pronounced microglia remodelling in response to CSS. There was a nominal increase in proximity between OPC and microglia in the BA in CSS mice, which did not survive FDR correction, and no such group difference in the mPFC (Figure 1D,E,G,H). Such proximity was not associated with increased cell-to-cell contact (Supplementary Figures S4B–C,F–H) or with increased overlap between OPCs and microglia, which could have hinted at phagocytosis-relevant events (Supplementary Figures S4D,E). Taken together, these data indicate a modest association between microglia and OPC density following CSS, without clear evidence for large-scale alterations in microglia morphology or microglia-OPC spatial organization. The limited robustness of the observed spatial effect is further emphasised by the lack of significance following FDR correction (Supplementary Table 1).

3.2 Microglia show a subtle increased ramification after CSS followed by an acute aversive experience

The exposure to chronic stressors can cause a permanent shift in the homeostasis and reactiveness of an organism (de Kloet et al., 2005), as supported, for instance, by the increased sensitivity to aversion, typically observed in CSS mice (Azzinnari et al., 2014; Sigrist et al., 2024; Poggi et al., 2025). We reasoned that this might be also reflected in differences in microglia and microglia-OPC histological changes following aversive challenge in CSS mice as compared to CON. Thus, we exposed mice to the CSS protocol followed by PAL and sacrificed the mice 90 min afterwards (Figure 2A). We focused on the BA and co-stained for OPC and microglia markers and estimated end-point proliferation using Ki-67. We observed a nominal reduction in the proportion of end-point proliferative OPCs in CSS mice vs. CON (Figure 2C), and a similar trend was detected when comparing the density of proliferative OPCs not normalised by the total density of OPCs (Figure 2B). However, this effect did not survive FDR correction (Supplementary Table 1). The overall cell density, the density of OPCs, and microglia were unaffected (Figures 2D–G). There was a correlation between microglia density and OPC density, but this was now specific to CON mice (Figures 2H,I). The effect persisted even after FDR correction, which supports the robustness of this observation. Quantification of microglia complexity via Sholl analysis revealed a trend toward an increased ramification of microglia in CSS + PAL mice as compared to CON + PAL mice (Figure 2J). This trend persisted after FDR correction. Further exploratory analysis, in which the Sholl analysis output was binned into a 20-**μ**m radial interval from the microglia cell body, did not indicate that the observed trend was concentrated within a specific radial range, but was rather homogeneously distributed across the analysed processes length (Figure 2K). There was no group difference with respect to proximity of microglia to OPCs (Figures 2L,M). Taken together, this suggests that the previously reported reduced proliferative capacity of OPCs in CSS mice [see *Experiment 1*, (Poggi et al., 2022)] might persist after exposure to an additional acute aversive challenge. Notably, the inclusion of a time-matched cohort with prior exposure to CSS but without conditioning (or with context exposure only) would be critical for drawing definitive conclusions on the synergic effects of CSS and PAL. However, qualitative integration of the collected evidence suggests that CSS might influence, although subtly, microglia responsiveness to an additional stressor.

3.3 Microglia and OPCs are unaffected by juvenile social isolation

Social isolation involves the absence of socio-positive stimulation, and as such can be considered a form of social stress (Wallace et al., 2009; Xiong et al., 2022). To evaluate the effects of social isolation on microglia and OPC histological properties, 5-week-old male mice were either single-housed (Social isolation, SI) or group-housed (social rearing, SR) for 4 weeks. In week 9, the mice were sacrificed and brain sections containing mPFC and BA were co-stained for markers of OPC, microglia, and Ki-67end-point proliferation. The densities of each of OPCs, proliferative OPCs, microglia and proliferative microglia were comparable between groups (Supplementary Figure S5). The morphology of microglia (Figures 3E, J) as well as their proximity to OPCs (Figures 3F,G,K,L) were unaffected by social isolation. Furthermore, there was no evidence for either SI or SR mice of any association between the density of microglia and of OPCs, neither for mPFC (Figures 3C,D) nor BA (Figure 3H,I). Notably, taken together, juvenile social isolation did not lead to any changes in OPCs or microglia, including those observed in response to CSS or to CSS + PAL.

4 Discussion

Social stress can lead to a broad and heterogeneous spectrum of oligodendrocyte lineage and myelin alterations. We hypothesised that such alterations co-occur with stress paradigm-specific.

microglia responses, which could potentially contribute to the heterogeneity of the (mal)adaptive response of the oligodendrocyte

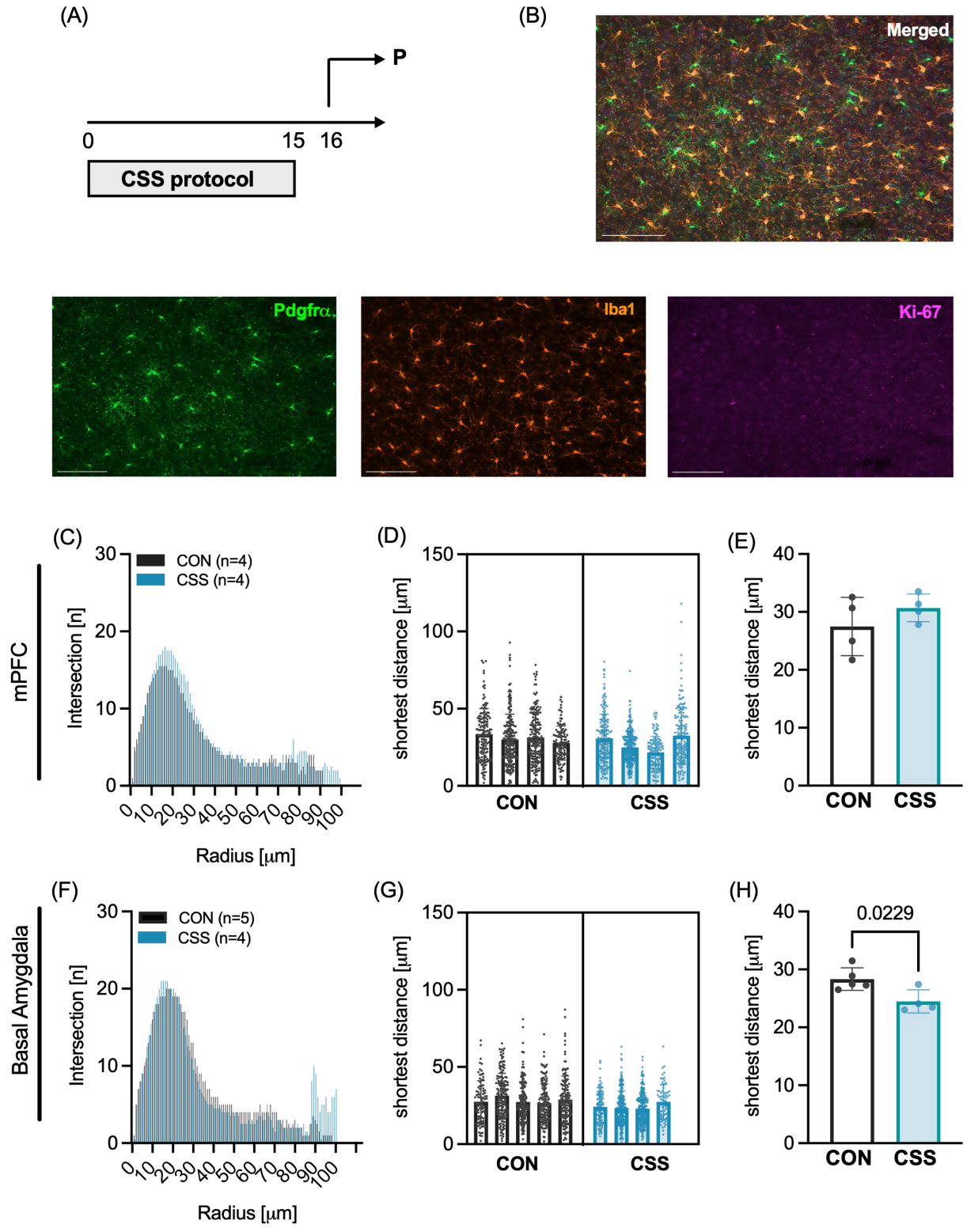


FIGURE 1
CSS does not alter microglia ramification in mPFC and BA and increases microglia-OPCs proximity in BA. **(A)** Experimental timeline (*P* = perfusion; timeline unit = day). **(B)** Representative micrographs (scale bar = 100 μm). **(C)** Microglia complexity estimated via Sholl analysis in mPFC (mixed-effects model, radius: F (2.358, 13.41) = 65.52, $p < 0.0001$; group: F (1, 6) = 0.9965 $p = 0.3567$, 95% C.I. [−3.540, 1.489]). **(D)** Shortest distance between OPCs and microglia in mPFC (single data points). **(E)** Mean shortest distance between OPCs and microglia in mPFC (t = 1.170, df = 6, $p = 0.2865$, 95% C.I. [−3.584, 10.01]). **(F)** Microglia complexity estimated via Sholl analysis in BA (mixed-effects model, radius: F (2.620, 17.24) = 109.2, $p < 0.0001$; group: F (1, 7) = 0.1935 $p = 0.6732$; 95% C.I. [−1.189, 1.733]). **(G)** Shortest distance between OPCs and microglia in BA (single data points). **(H)** Mean shortest distance between OPCs and icroglia in BA (unpaired t-test, $t = 2.904$, df = 7, $p = 0.0229$, 95% C.I. [−6.969, −0.7136]). Data are presented as the mean (**C**, **F**) or mean ± S.D. **(D, E, G, H)** (CON, $n = 45$; CSS, $n = 4$; 2 brain sections per mouse per brain region; n of cells >100/mouse).

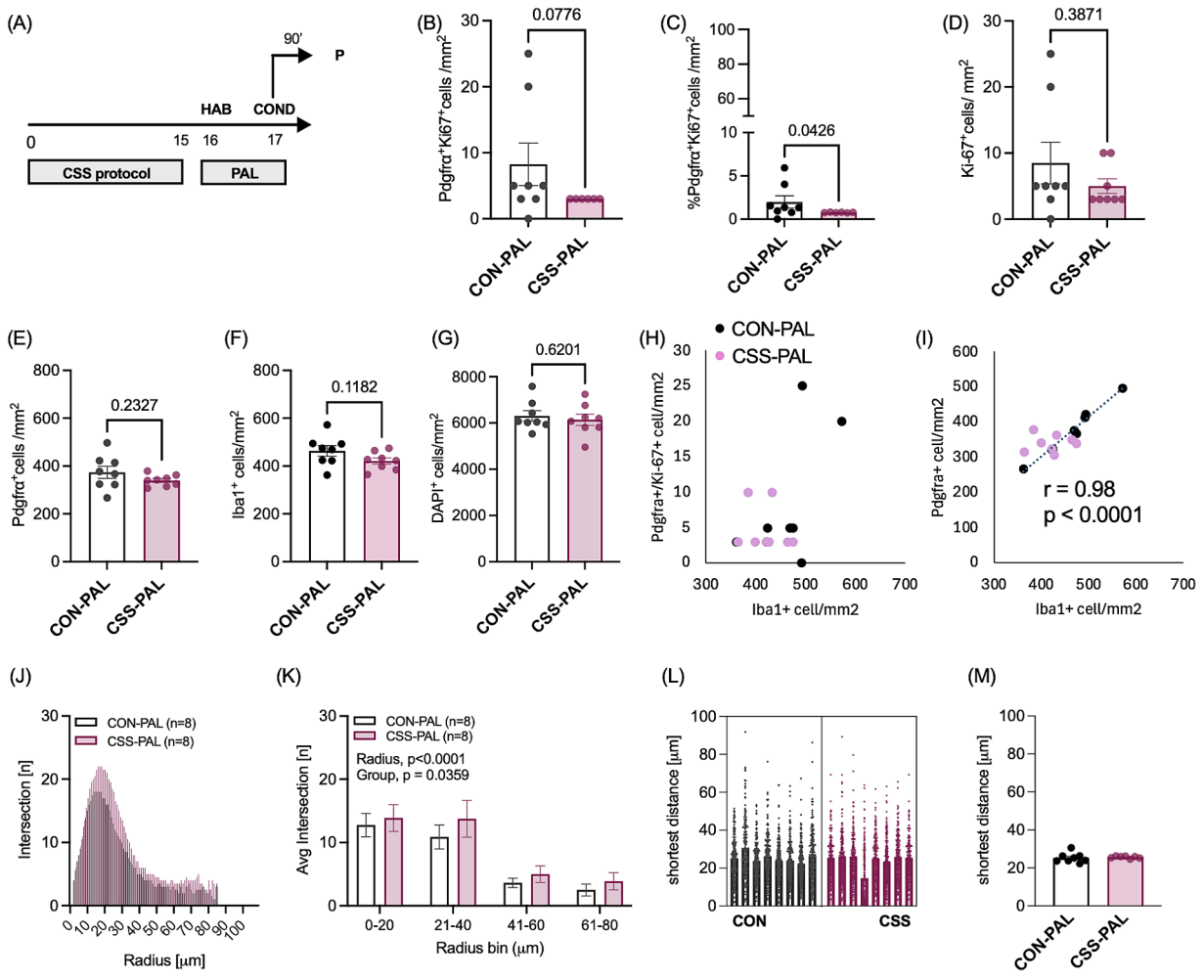


FIGURE 2
CSS-PAL reduces end-point proliferative OPCs and shows a subtle increase in microglia complexity in BA, whilst OPCs density correlates positively with microglia density in CON-PAL and not CSS-PAL mice. **(A)** Experimental timeline (HAB = Habituation, COND = conditioning, P = perfusion; Timeline unit = day). **(B)** Density of end-point proliferative OPCs (Pdgfrα$^+$/Ki-67$^+$, Mann Whitney test, U = 12, p = 0.0776, 95.74% C.I. [-17.00, 0.00]). **(C)** Percentage of end-point proliferative OPCs with respect to the overall OPC density (Pdgfrα$^+$/Ki-67$^+$ of Pdgfrα$^+$, Mann Whitney test, U = 8, p = 0.0426, 95.74% C.I. [−3.290, 0.0100]). **(D)** Density of end-point proliferative cells (Ki-67$^+$, Mann Whitney test, U = 23.5, p = 0.3871, 95.01% C.I. [−15.00, 3.00]). **(E)** Density of OPCs (Pdgfrα$^+$, Unpaired t test with Welch's correction, t = 1.284, df = 8.589, p = 0.2327, 95% C.I. [−95.04, 26.54]). **(F)** Density of microglia (Iba1$^+$, Unpaired t test, t = 1.664, df = 14 p = 0.1182, 95% C.I. [−98.12, 12.37]). **(G)** Overall cell density (DAPI$^+$, Unpaired t test, t = 0.5070, df = 14 p = 0.6201, 95% C.I. [−877.4, 541.9]). **(H)** Density of microglia (Iba1$^+$) vs. density of proliferative OPCs (Pdgfrα$^+$/Ki-67$^+$) in the BA of CON (Pearson R, r = 0.6016, p = 0.1146, 95% C.I. [−0.1789, 0.9174]) and CSS (Pearson R, r = −0.2091, p = 0.6193, 95% C.I. [−0.7964, 0.5812]) mice. **(I)** Density of microglia (Iba1$^+$) vs. density of OPCs (Pdgfrα$^+$) in the BA of CON (Pearson R, r = 0.9898, p < 0.0001, 95% C.I. [0.9427, 0.9982]) and CSS (Pearson R, r = 0.05576, p = 0.8957, 95% C.I. [−0.67554, 0.7317]) mice. **(J)** Microglia complexity estimated via Sholl analysis in BA (Mixed-effects model, radius: F (2.779, 36.06) = 261.1, p < 0.0001; group: F (1, 14) = 4.100, p = 0.0624; radius × group: F (2.779, 36.06) = 1.450, p = 0.2455, 95% C.I. of difference [−3.161, 0.09101]). **(K)** Microglia complexity estimated via binned Sholl analysis in BA (Two-way RM ANOVA, radius: F (3, 42) = 338.3, p < 0.0001; group: F (1, 14) = 5.389, p = 0.0359, 95% C.I. of difference [−3.247, −0.1283]). **(L)** Shortest distance between OPCs and Microglia (single datapoint). **(M)** Average shortest distance between OPCs and Microglia (Unpaired t test, t = 0.3605, df = 13, p = 0.7243, 95% C.I. [−1.806, 2.529]). Data are presented as the mean **(H, I)** or the mean ± S.D. (BG, JM) (CON, n = 8; CSS, n = 8; 1 brain sections per mouse per brain region).

lineage. In the current study, we assessed: (1) the density and proliferation rate of microglia and OPCs; (2) the spatial relationship between microglia and OPCs; and (3) microglia morphological complexity as an indication of their state in the context of different social stress protocols. We gathered preliminary yet integrative histological evidence that different social stress setups might lead to subtle divergent microglial histological responses, which do not seem to robustly associate with the examined OPC histological features. The summary of the results is reported in Table 1.

A recent meta-analysis revealed that chronic stress leads to reduction of oligodendrocyte transcripts in the mPFC of male mice (Xiong et al., 2026). However, findings beyond simple transcript analysis have reported heterogeneous outcomes, including increase (Laine et al., 2018; Poggi et al., 2022), decrease (Lehmann et al., 2017; Bonnefil et al., 2019; Kokkosis et al., 2022) or no changes in oligodendrocyte lineage or myelin content (Cathomas et al., 2019; Poggi et al., 2022) in mPFC and amygdala. Similarly, a previous study showed that focal demyelination in mPFC leads to social behaviour deficits, typically observed after CSD (Bonnefil et al., 2019). Collectively, these findings raise the question of whether the direction of the changes in oligodendrocyte lineage and myelin status (loss vs. gain) might be an overly simplistic metric of brain circuit (dys)function in response to stress and that social stress-induced dysregulation of oligodendrocyte lineage dynamics and myelin remodelling may occur through multiple

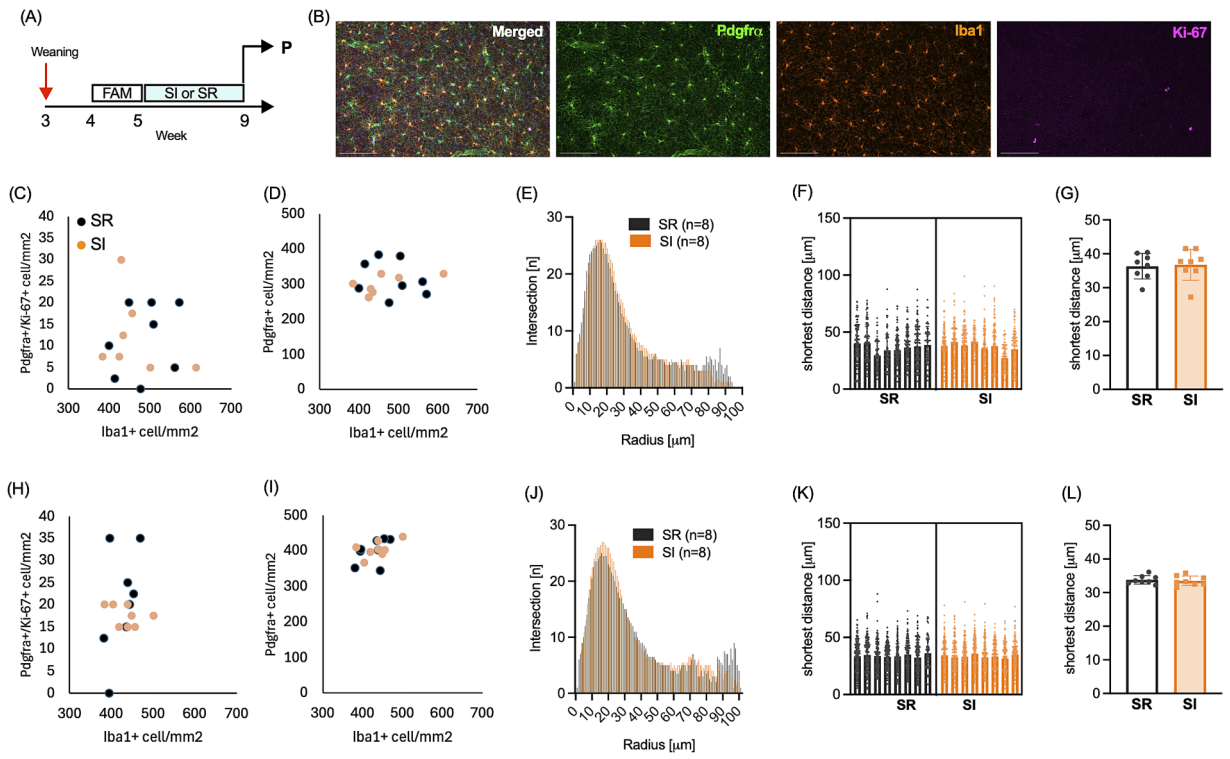


FIGURE 3
Juvenile social isolation does not affect microglia morphology or proximity to OPCs and does not associate with OPC density-microglia density correlation **(A)** Experimental timeline: (FAM = familiarization phase; SI = social isolation; SR = standard rearing; P = perfusion). **(B)** Representative micrographs (scale bar = 100 µm). **(C)** Density of microglia (Iba1$^+$) vs. density of proliferative OPCs (Pdgfrα^+/Ki-67$^+$) in the mPFC of SR (Pearson *R*, *r* = 0.2819, *p* = 0.4988, 95% C.I. [−0.5276, 0.8231]) and SI (Pearson *R*, *r* = -0.3557, *p* = 0.4336, 95% C.I. [−0.8745, 0.5427]) mice. **(D)** Density of microglia (Iba1$^+$) vs. density of OPCs (Pdgfrα^+) in the mPFC of SR (Pearson *R*, *r* = −0.2765, *p* = 0.5073, 95% C.I. [−0.8212, 0.5318]) and SI (Pearson *R*, *r* = 0.6190, *p* = 0.1383, 95% C.I. [−0.2512, 0.9358]) mice. **(E)** Microglia complexity estimated via Sholl analysis in mPFC (Mixed-effects model, radius: F (2.344, 30.11) = 114.6, $p < 0.0001$; group: F (1, 14) = 0.9490, p = 0.3465, 95% C.I. of difference [−3.509, 1.317]). **(F)** Shortest distance between OPCs and Microglia in mPFC (single data points). **(G)** Average shortest distance between OPCs and icroglia in mPFC (Unpaired *t* test, *t* = 0.2079, df = 14, *p* = 0.8383, 95% C.I. [−4.057, 4.928]). **(H)** Density of microglia (Iba1$^+$) vs. density of proliferative OPCs (Pdgfrα^+/Ki-67$^+$) in the BA of SR (Pearson *R*, *r* = 0.4806, *p* = 0.2281, 95% C.I. [−0.3389, 0.8854]) and SI (Pearson *R*, *r* = −0.3784, *p* = 0.3553, 95% C.I. [−0.8551, 0.4449]) mice. **(I)** Density of microglia (Iba1$^+$) vs. density of OPCs (Pdgfrα^+) in the BA of SR (Pearson *R*, *r* = 0.4762, *p* = 0.2329, 95% C.I. [−0.3439, 0.8842]) and SI (Pearson *R*, *r* = 0.5766, *p* = 0.1346, 95% C.I. [−0.2158, 0.9111]) mice. **(J)** Microglia complexity estimated via Sholl analysis in BA of SR vs. SI mice (Mixed-effects model, radius: F (2.622, 33.36) = 148.1, $p < 0.0001$; group: F (1, 14) = 0.2016, p = 0.6603, 95% C.I. of difference [−2.789, 1.824]). **(K)** Shortest distance between OPCs and Microglia in BA (single data points). **(L)** Average shortest distance between OPCs and icroglia in BA (Unpaired *t* test, *t* = 0.4077, df = 14, *p* = 0.6896, 95% C.I. [−1.717, 1.168]). Data are presented as mean **(C, D, H, I)** or mean ± S.D. (EG, JL) (SR, *n* = 8; SI, *n* = 7–8; 1 brain sections per mouse per brain region).

biological trajectories, which might converge in similar behavioural alterations.

Multiple independent studies reported that microglia are implicated in mounting (an inflammatory) response to chronic social stress (Hellwig et al., 2016; Picard et al., 2021; Brás et al., 2022; Orso et al., 2023; Kokkosis et al., 2024; Madeira et al., 2025). Additionally, microglia have been reported to regulate the function and status of the oligodendrocyte lineage and myelin in health and diseases (Santos and Fields, 2021; McNamara et al., 2023). Interestingly, our exploratory over-representation and microglia-pathway enrichment analyses—based exclusively on differentially expressed genes ($p \leq 0.05$) in two independent gene-expression datasets—highlighted only limited overlap with respect to changes in microglia pathways between stress protocols associated with myelin loss or myelin gain. Although these results should be interpreted with caution given the different employed gene-expression platforms (microarray vs. bulk RNA-seq) and the lack of causal evidence, they align with the hypothesis of a stress paradigm-specific microglia response.

It was reported that CSD protocol leads to an increase of CD68 marker and a pronounced microglia activation in stress susceptible mice (Lehmann et al., 2016, 2018) and it was speculated that activated microglia could be implicated in the phagocytosis of myelin debris (Lehmann et al., 2016, 2018). RSDS studies demonstrated that loss of myelin is associated with increased microglia proliferation and pronounced inflammatory response (Kokkosis et al., 2022; Madeira et al., 2025). In contrast, these phenomena were not observed in CSS studies (Poggi et al., 2022). Indeed, although CSS induced changes in inflammatory markers (Azzinnari et al., 2014; Bergamini et al., 2018), it did not alter Iba1$^+$/CD68$^+$ microglia density or proliferation (Poggi et al., 2022). When performing new analyses on the previously published histological dataset, we observed that, while OPC and microglia densities were comparable between CSS and CON mice (Poggi et al., 2022), microglia density correlated with OPC density in mPFC and, to a lesser extent, in amygdala, in CSS mice specifically. Additionally, proliferative OPC density correlated negatively with microglia density in both regions. These correlative patterns were observed, at least in part, in an independent CSS experiment (*Experiment 2*). It should be noted that Ki-67 staining—in contrast to EdU labelling—allows exclusively for the assessment of end-point proliferation. Therefore, while the output of *Experiment 2* suggests that the density of end-point

TABLE 1 Result summary.

Experiment ID	Original manuscript	Sample size	Sex/ age	Microglia		OPCs	OPC-Microglia	
				Density	Sholl analysis	Proliferation	Density correlation	Proximity
Experiment 1 | EdU - CSS	Poggi et al., 2022	CON, $n = 12$; CSS, $n = 14$	M/10-week-old			↓ in BA and mPFC	In mPFC of CSS mice: - Microglia↑ = OPC↑ - Microglia ↑ = proliferative OPCs ↓ In BA of CSS mice: - Microglia ↑ = proliferative OPCs ↓	
Experiment 2 | CSS	NA	CON, $n = 5$; CSS, $n = 5$;	M/10-week-old				In mPFC of CSS mice: - Microglia ↕ = OPCs ↕ In BA of CSS mice: - Microglia ↕ = OPCs ↕	In BA of CSS mice: - ↑ Microglia-OPC
Experiment 3 | CSS + PAL	NA	CON + PAL, $n = 8$; CSS + PAL, $n = 8$;	M/10-week-old		↑ intersection CSS in BA	↓ in BA of CSS	In BA of CON mice: - Microglia↑ = OPC↑	
Juvenile social isolation	Wicki et al., 2026	SR, $n = 8$; SI, $n = 8$;	M/9-week-old					

Full line arrow ($p < 0.05$), dashed arrow (trend, $p < 0.1$). EdU, 5-ethynyl 2'-deoxyuridine; CSS, chronic social stress; CON, control; PAL, Pavlovian Aversion Learning; BA, basal amygdala; mPFC, medial prefrontal cortex. The summary is based on nominal p-values. Statistical significance following Benjamini–Hochberg false discovery rate (BH-FDR) correction is reported in Supplementary Table 1.

proliferative OPCs does not negatively correlate with the density of microglia, it does not permit full replication and validation of the output observed in *Experiment 1*. Also, it is critical to point out that only part of the observed effects survived FDR correction, highlighting the limited robustness and preliminary nature of the current observations.

A functional relationship between microglia and OPCs is supported by developmental and disease studies. During development, microglia regulate the proliferation of OPCs (Taylor et al., 2010) and directly determine white matter OPCs density (Nemes-Baran et al., 2020)—with their depletion leading to the reduction of OPCs density (Hagemeyer et al., 2017). In both clinical and preclinical CNS demyelination studies, OPC density correlates with microglia density, further supporting an inter-relationship between these cell populations (Wolswijk, 2002; Ma et al., 2024). In the context of multiple sclerosis, microglia have been proven essential for OPCs recruitment, proliferation and differentiation at the lesions and for promoting tissue regeneration through the secretion of anti-inflammatory cytokines and growth factors (Miron et al., 2013; Sherafat et al., 2021). Nevertheless, the correlative nature of our findings precludes definitive conclusions regarding causality, directionality, or the precise mechanisms underlying putative microglia-OPC histological inter-relationship. Indeed, an OPC-to-microglia communication (Liu and Aguzzi, 2020) as well as a coregulation of microglia and OPCs by a common upstream mechanism (e.g., neuronal activity), which does not entail OPC-microglia crosstalk, remain plausible alternative mechanisms to investigate.

To start dissecting the potential biological processes that might underlie the observed correlation, we carried out additional histological assessments of microglia and OPCs following CSS protocol. We detected only a nominal increased proximity between microglia and OPCs in the BA of CSS mice, while microglial morphology remained unchanged. Although morphology alone does not resolve functional or transcriptional states, these observations do not provide evidence for a substantial remodelling of microglia morphology in response to CSS and might speak against the inflammatory microglia phenotype described in CSD and RSDS models (Lehmann et al., 2016, 2018, 2019; Kokkosis et al., 2024; Madeira et al., 2025). Also, the lack of CSS effects on microglia-OPC direct contact or overlapping, despite the nominal increased microglia-OPC proximity in BA, further speaks against the onset of microglia-mediated phagocytosis-relevant events impacting on the OPCs. It should be noted that, while our histological assessment is suggestive of the absence of clear and pronounced phagocytosis-relevant events in CSS, it does not provide a direct measure of phagocytic activity. Whether this putative non-inflammatory phenotype of microglia plays a role in the oligodendrocyte lineage response to CSS cannot be concluded from the current findings

and remains an open question. Future studies combining cell-specific functional perturbation approaches with high-resolution molecular profiling of both OPCs and microglia will be necessary to further dissect the phenotype of these cell populations, and to be certain about the absence (or presence) of any inter-relationship between them, in response to CSS.

A tendency to an increased microglia ramification was detected in mice 90 min after the exposure to PAL in the BA of CSS mice. Studies of the kinetics of microglia morphology and motility show that filopodia extension can initiate within minutes after injury or perturbation (Wagner et al., 2024). Therefore, this speed of reaction would be coherent with the morphological remodelling observed in CSS mice 90 min after aversion learning, but the biological significance of this phenotype remains unclear. Hyperramified microglia have been described in preclinical models of chronic stress (Hellwig et al., 2016), alcoholism (Socodato et al., 2020), and of PTSD (Smith et al., 2019), in stress (Hinwood et al., 2013) and neurodegeneration (Bisht et al., 2016). Also, *in vivo* preclinical studies have shown that highly ramified microglia are associated with higher anxiety and depression-relevant symptoms, as well as reduced social exploration and less proactive challenge-coping behaviour (Maras et al., 2022). Notably, increased microglial ramification can be induced *ex-vivo* by neuronal activity and synaptic plasticity-related paradigms, including long-term potentiation and AMPA and NMDA stimulation (Fontainhas et al., 2011; Pfeiffer et al., 2016). Since CSS mice generally display enhanced aversion learning (Poggi et al., 2025), it is conceivable that the subtle increased ramification of microglia post-PAL might reflect an increased microglia responsiveness to aversion challenge. This hypothesis needs, nevertheless, further validation in a separate cohort where the individual fear response magnitude could be directly associated with the microglia morphological rearrangements, and where microglia markers could be assessed to determine the cell functional state. This morphological change in microglia co-occurred with a nominal reduction of endpoint OPC proliferation. However, whether these two phenomena are biologically interconnected cannot be deduced from the current dataset and remains an open question for future studies. In this dataset we detected an exceptionally robust correlation between microglia and OPC densities in CON mice exposed to aversion learning, which survived FDR correction. This might further highlight a substantial change in the aversion response pattern of microglia after CSS and possibly hint once more at a potential interdependence between microglia and OPCs in the response to aversive experience in otherwise non-stressed mice.

To further investigate the heterogeneity of the oligodendrocyte and microglia response to social aversion, we complemented our approach by analysing microglia and OPC histological properties in a cohort of socially isolated juvenile male mice. Independent studies have shown that social isolation induces anxiety- and anhedonia-like symptoms (Wallace et al., 2009), and social deficits (Liu et al., 2012; Makinodan et al., 2012). Also, our social isolation protocol, applied from P35 to P56, led to impairment of long-term memory of visual stimulus–reward/non-reward associations (Wicki et al., 2026). Notably, although we did not directly assess this in our cohort, independent studies have also shown that juvenile and adult social isolation reduce myelin-related transcripts and myelin content (Liu et al., 2012; Makinodan et al., 2012; Zhang et al., 2023) and impair OPC and early oligodendrocyte maturation in the mPFC (Zhang et al., 2022, 2023). In the current study, juvenile social isolation did not impact on either the density or the proliferation of OPCs and microglia, the morphology of microglia or their proximity to OPCs, and also not on their correlation, in mPFC or BA. Some studies employing either shorter or time-shifted social isolation protocols identified a higher Iba1 staining intensity (Ferrara et al., 2022) and changes in microglia complexity in cortical regions and in the amygdala (Ferrara et al., 2022). While our findings do not fully rule out the involvement of these cell populations in the response to social isolation, they highlight, once again, the heterogeneous effects of diverse social aversive experience on the oligodendrocyte lineage and microglia, despite rather similar behavioural outcomes.

It is important to note that our study presents three main limitations. First, while a few nominally significant effects were observed, most of them did not survive FDR correction. This further highlights the preliminary and exploratory nature of the study and indicates that our results warrant cautious interpretation and require future additional validation in independent cohorts. Second, the employed cohorts include exclusively male mice, limiting the relevance of the output to a biased subset of individuals of the general population. Given the documented sex-related differences in glia biology (Marin-Husstege et al., 2004; Patel et al., 2013; Nesbitt et al., 2025), it is conceivable that a substantial different picture might derive from analysis of female mice. Third, the current study provides an exploratory integration of findings from independent stress-related cohorts and does not constitute a systematic and direct cross-paradigm comparison. In conclusion, despite the indicated limitations, our findings provide histological evidence that subtle microglial and OPC responses vary across different (social) stress paradigms. Importantly, rather than supporting a uniform microglia-mediated regulation of social stress-induced oligodendrocyte lineage alterations, our data point toward the existence of diverse microglial and oligodendrocyte lineage responses that may accompany similar stress-induced behavioural outcomes. Critically, the implementation of gene expression analysis and functional assays would be essential to further elucidate the mechanisms underlying the heterogeneous effects of social stress on microglia and OPCs pathophysiology. Understanding how distinct social stress experiences shape microglia, the oligodendrocyte lineage and their potential interrelationship is therefore essential for deciphering the biological basis of stress adaptation and maladaptation.

Data availability statement

The raw data supporting the conclusions of this article will be made available by the authors, without undue reservation.

Ethics statement

The animal study was approved by Veterinary Office of Canton Zurich (licenses: ZH-149/2015, ZH-155/2018 ZH093/2019, ZH-174/2021, and ZH-038/2022). The study was conducted in accordance with the local legislation and institutional requirements.

Author contributions

SGR: Writing – review & editing, Methodology, Investigation, Writing – original draft, Formal analysis, Data curation, Visualization, Validation. SW: Methodology, Writing – review & editing, Investigation. SS: Methodology, Writing – review & editing, Investigation. DEH: Writing – review & editing, Investigation, Methodology. MBM: Resources, Writing – review & editing, Supervision. CRP: Supervision, Project administration, Resources, Funding acquisition, Writing – review & editing. MJS: Writing – review & editing, Resources, Funding acquisition. GP: Supervision, Writing – original draft, Methodology, Conceptualization, Investigation, Visualization, Project administration, Formal analysis, Validation, Writing – review & editing, Data curation.

Funding

The author(s) declared that financial support was received for this work and/or its publication. This publication is supported by the Johannes Gutenberg University Mainz Open-Access publication funding. MS was supported by the Werner Reichenberger Foundation.

Acknowledgments

We are grateful to Bozana Heil, Agnieszka Mojek, and Alex Osei for animal care, to Hannes Sigrist, Julia Deuster and Jennifer Kluepfel for technical support, to Verena Opitz for administrative support, to the Center for Microscopy and Image Analysis, University of Zurich, Christof Richert and Bastian Hülsmann at the Light Microscopy Core Facilities, University of Mainz, for assistance and support microscopy image acquisition.

Conflict of interest

The author(s) declared that this work was conducted in the absence of any commercial or financial relationships that could be construed as a potential conflict of interest.

The author MJS declared that they were an editorial board member of Frontiers, at the time of submission. This had no impact on the peer review process and the final decision.

Generative AI statement

The author(s) declared that Generative AI was used in the creation of this manuscript. Generative AI was used to support python scripting and for refining grammar, structure and readability of the manuscript.

Any alternative text (alt text) provided alongside figures in this article has been generated by Frontiers with the support of artificial intelligence and reasonable efforts have been made to ensure accuracy, including review by the authors wherever possible. If you identify any issues, please contact us.

Publisher's note

All claims expressed in this article are solely those of the authors and do not necessarily represent those of their affiliated organizations, or those of the publisher, the editors and the reviewers. Any product that may be evaluated in this article, or claim that may be made by its manufacturer, is not guaranteed or endorsed by the publisher.

Supplementary material

The Supplementary material for this article can be found online at: https://www.frontiersin.org/articles/10.3389/fncel.2026.1928157/full#supplementary-material

References

Allsop, S. A., Wichmann, R., Mills, F., Burgos-Robles, A., Chang, C. J., Felix-Ortiz, A. C., et al. (2018). Corticoamygdala transfer of socially derived information gates observational learning. *Cell* 173, 1329–1342.e18. doi: 10.1016/j.cell.2018.04.004

Azzinnari, D., Sigrist, H., Staehli, S., Palme, R., Hildebrandt, T., Leparc, G., et al. (2014). Mouse social stress induces increased fear conditioning, helplessness and fatigue to physical challenge together with markers of altered immune and dopamine function. *Neuropharmacology* 85, 328–341. doi: 10.1016/j.neuropharm.2014.05.039

Bergamini, G., Cathomas, F., Auer, S., Sigrist, H., Seifritz, E., Patterson, M., et al. (2016). Mouse psychosocial stress reduces motivation and cognitive function in operant reward tests: a model for reward pathology with effects of agomelatine. *Eur. Neuropsychopharmacol.* 26, 1448–1464. doi: 10.1016/j.euroneuro.2016.06.009

Bergamini, G., Mechtersheimer, J., Azzinnari, D., Sigrist, H., Buerge, M., Dallmann, R., et al. (2018). Chronic social stress induces peripheral and central immune activation, blunted mesolimbic dopamine function, and reduced reward-directed behaviour in mice. *Neurobiol. Stress* 8, 42–56. doi: 10.1016/j.ynstr.2018.01.004

Bisht, K., Sharma, K. P., Lecours, C., Gabriela Sánchez, M., El Hajj, H., Milior, G., et al. (2016). Dark microglia: a new phenotype predominantly associated with pathological states. *Glia* 64, 826–839. doi: 10.1002/glia.22966

Bonnefil, V., Dietz, K., Amatruda, M., Wentling, M., Aubry, A. V., Dupree, J. L., et al. (2019). Region-specific myelin differences define behavioral consequences of chronic social defeat stress in mice. *eLife* 8, 1–13. doi: 10.7554/eLife.40855

Brás, J. P., Guillot de Suduiraut, I., Zanoletti, O., Monari, S., Meijer, M., Grosse, J., et al. (2022). Stress-induced depressive-like behavior in male rats is associated with microglial activation and inflammation dysregulation in the hippocampus in adulthood. *Brain Behav. Immun.* 99, 397–408. doi: 10.1016/j.bbi.2021.10.018

Cathomas, F., Azzinnari, D., Bergamini, G., Sigrist, H., Buerge, M., Hoop, V., et al. (2019). Oligodendrocyte gene expression is reduced by and influences effects of chronic social stress in mice. *Genes Brain Behav.* 18, e12475–e12414. doi: 10.1111/gbb.12475

d'Arbeloff, T. C., Kim, M. J., Knodt, A. R., Radtke, S. R., Brigidi, B. D., and Hariri, A. R. (2018). Microstructural integrity of a pathway connecting the prefrontal cortex and amygdala moderates the association between cognitive reappraisal and negative emotions. *Emotion* 18, 912–915. doi: 10.1037/emo0000447

de Kloet, E. R., Joëls, M., and Holsboer, F. (2005). Stress and the brain: from adaptation to disease. *Nat. Rev. Neurosci.* 6, 463–475. doi: 10.1038/nrn1683

Díez-Solinska, A., De Miguel, Z., Azkona, G., and Vegas, O. (2024). Behavioral coping with chronic defeat stress in mice: a systematic review of current protocols. *Neurobiol. Stress* 33:100689. doi: 10.1016/j.ynstr.2024.100689

Ferrara, N. C., Trask, S., Yan, L., Padival, M., Helmstetter, F. J., and Rosenkranz, J. A. (2022). Isolation driven changes in Iba1-positive microglial morphology are associated with social recognition memory in adults and adolescents. *Neurobiol. Learn. Mem.* 192:107626. doi: 10.1016/j.nlm.2022.107626

Fontainhas, A. M., Wang, M., Liang, K. J., Chen, S., Mettu, P., Damani, M., et al. (2011). Microglial morphology and dynamic behavior is regulated by ionotropic glutamatergic and GABAergic neurotransmission. *PLoS One* 6:e15973. doi: 10.1371/journal.pone.0015973

Fuertig, R., Azzinnari, D., Bergamini, G., Cathomas, F., Sigrist, H., Seifritz, E., et al. (2016). Mouse chronic social stress increases blood and brain kynurenine pathway activity and fear behaviour: both effects are reversed by inhibition of indoleamine 2,3-dioxygenase. *Brain Behav. Immun.* 54, 59–72. doi: 10.1016/j.bbi.2015.12.020

García-Cabezas, M., and Barbas, H. (2017). Anterior cingulate pathways may affect emotions through orbitofrontal cortex. *Cereb. Cortex* 27, 4891–4910. doi: 10.1093/cercor/bhw284

Golden, S. A., Covington, H. E., Berton, O., and Russo, S. J. (2011). A standardized protocol for repeated social defeat stress in mice. *Nat. Protoc.* 6, 1183–1191. doi: 10.1038/nprot.2011.361

Grandjean, J., Azzinnari, D., Seuwen, A., Sigrist, H., Seifritz, E., Pryce, C. R., et al. (2016). Chronic psychosocial stress in mice leads to changes in brain functional connectivity and metabolite levels comparable to human depression. *NeuroImage* 142, 544–552. doi: 10.1016/j.neuroimage.2016.08.013

Hagemeyer, N., Hanft, K. M., Akriditou, M. A., Unger, N., Park, E. S., Stanley, E. R., et al. (2017). Microglia contribute to normal myelinogenesis and to oligodendrocyte progenitor maintenance during adulthood. *Acta Neuropathol.* 134, 441–458. doi: 10.1007/s00401-017-1747-1

Hellwig, S., Brioschi, S., Dieni, S., Frings, L., Masuch, A., Blank, T., et al. (2016). Altered microglia morphology and higher resilience to stress-induced depression-like behavior in CX3CR1-deficient mice. *Brain Behav. Immun.* 55, 126–137. doi: 10.1016/j.bbi.2015.11.008

Hinwood, M., Tynan, R. J., Charnley, J. L., Beynon, S. B., Day, T. A., and Walker, F. R. (2013). Chronic stress induced remodeling of the prefrontal cortex: structural re-organization of microglia and the inhibitory effect of minocycline. *Cereb. Cortex* 23, 1784–1797. doi: 10.1093/cercor/bhs151

Jao, J., and Ciernia, A. V. (2021). MGEnrichment: a web application for microglia gene list enrichment analysis. *PLoS Comput. Biol.* 17:e1009160. doi: 10.1371/journal.pcbi.1009160

Kalafatakis, I., and Karagogeos, D. (2021). Oligodendrocytes and microglia: key players in myelin development, damage and repair. *Biomolecules* 11:1058. doi: 10.3390/biom11071058

Kokkosis, A. G., Madeira, M. M., Hage, Z., Valais, K., Koliatsis, D., Resutov, E., et al. (2024). Chronic psychosocial stress triggers microglial-/macrophage-induced inflammatory responses leading to neuronal dysfunction and depressive-related behavior. *Glia* 72, 111–132. doi: 10.1002/glia.24464

Kokkosis, A. G., Madeira, M. M., Mullahy, M. R., and Tsirka, S. E. (2022). Chronic stress disrupts the homeostasis and progeny progression of oligodendroglial lineage cells, associating immune oligodendrocytes with prefrontal cortex hypomyelination. *Mol. Psychiatry* 27, 2833–2848. doi: 10.1038/s41380-022-01512-y

Koskinen, M. K., Laine, M., Abdollahzadeh, A., Gigliotta, A., Mazzini, G., Journée, S., et al. (2023). Node of Ranvier remodeling in chronic psychosocial stress and anxiety. *Neuropsychopharmacology* 48, 1532–1540. doi: 10.1038/s41386-023-01568-6

Laine, M. A., Trontti, K., Misiewicz, Z., Sokolowska, E., Kulesskaya, N., Heikkinen, A., et al. (2018). Genetic control of myelin plasticity after chronic psychosocial stress. *eNeuro* 5:ENEURO.0166-18.2018. doi: 10.1523/ENEURO.0166-18.2018

Lander, S. S., Linder-Shacham, D., and Gaisler-Salomon, I. (2017). Differential effects of social isolation in adolescent and adult mice on behavior and cortical gene expression. *Behav. Brain Res.* 316, 245–254. doi: 10.1016/j.bbr.2016.09.005

Lehmann, M. L., Cooper, H. A., Maric, D., and Herkenham, M. (2016). Social defeat induces depressive-like states and microglial activation without involvement of peripheral macrophages. *J. Neuroinflammation* 13:224. doi: 10.1186/s12974-016-0672-x

Lehmann, M. L., Weigel, T. K., Cooper, H. A., Elkahloun, A. G., Kigar, S. L., and Herkenham, M. (2018). Decoding microglia responses to psychosocial stress reveals blood-brain barrier breakdown that may drive stress susceptibility. *Sci. Rep.* 8:11240. doi: 10.1038/s41598-018-28737-8

Lehmann, M. L., Weigel, T. K., Elkahloun, A. G., and Herkenham, M. (2017). Chronic social defeat reduces myelination in the mouse medial prefrontal cortex. *Sci. Rep.* 7, 1–13. doi: 10.1038/srep46548

Lehmann, M. L., Weigel, T. K., Poffenberger, C. N., and Herkenham, M. (2019). The behavioral sequelae of social defeat require microglia and are driven by oxidative stress in mice. *J. Neurosci.* 39, 5594–5605. doi: 10.1523/JNEUROSCI.0184-19.2019

Liu, J., Dietz, K., DeLoyht, J. M., Pedre, X., Kelkar, D., Kaur, J., et al. (2012). Impaired adult myelination in the prefrontal cortex of socially isolated mice. *Nat. Neurosci.* 15, 1621–1623. doi: 10.1038/nn.3263

Liu, Y., and Aguzzi, A. (2020). NG2 glia are required for maintaining microglia homeostatic state. *Glia* 68, 345–355. doi: 10.1002/glia.23721

Ma, D., Zhang, H., Yin, L., Xu, H., Wu, L., Shaji, R., et al. (2024). Human iPSC-derived endothelial cells promote CNS remyelination via BDNF and mTORC1 pathway. *Glia* 72, 133–155. doi: 10.1002/glia.24466

Madeira, M. M., Hage, Z., Kokkosis, A. G., Nnah, K., Guzman, R., Schappell, L. E., et al. (2025). Oligodendroglia are primed for antigen presentation in response to chronic stress-induced microglial-derived inflammation. *Glia* 73, 1130–1147. doi: 10.1002/glia.24661

Madur, L., Ineichen, C., Bergamini, G., Greter, A., Poggi, G., Cuomo-Haymour, N., et al. (2023). Stress deficits in reward behaviour are associated with and replicated by dysregulated amygdala-nucleus accumbens pathway function in mice. *Commun. Biol.* 6:422. doi: 10.1038/s42003-023-04811-4

Makinodan, M., Rosen, K. M., Ito, S., and Corfas, G. (2012). A critical period for social experience-dependent oligodendrocyte maturation and myelination. *Science* 337, 1357–1360. doi: 10.1126/science.1220845

Maras, P. M., Hebda-Bauer, E. K., Hagenauer, M. H., Hilde, K. L., Blandino, P., Watson, S. J., et al. (2022). Differences in microglia morphological profiles reflect divergent emotional temperaments: insights from a selective breeding model. *Transl. Psychiatry* 12:105. doi: 10.1038/s41398-022-01821-4

Marin-Husstege, M., Muggironi, M., Raban, D., Skoff, R. P., and Casaccia-Bonnefil, P. (2004). Oligodendrocyte progenitor proliferation and maturation is differentially regulated by male and female sex steroid hormones. *Dev. Neurosci.* 26, 245–254. doi: 10.1159/000082141

McNamara, N. B., Munro, D. A. D., Bestard-Cuche, N., Uyeda, A., Bogie, J. F. J., Hoffmann, A., et al. (2023). Microglia regulate central nervous system myelin growth and integrity. *Nature* 613, 120–129. doi: 10.1038/s41586-022-05534-y

Miron, V. E., Boyd, A., Zhao, J.-W., Yuen, T. J., Ruckh, J. M., Shadrach, J. L., et al. (2013). M2 microglia and macrophages drive oligodendrocyte differentiation during CNS remyelination. *Nat. Neurosci.* 16, 1211–1218. doi: 10.1038/nn.3469

Murphy, E. R., Barch, D. M., Pagliaccio, D., Luby, J. L., and Belden, A. C. (2016). Functional connectivity of the amygdala and subgenual cingulate during cognitive reappraisal of emotions in children with MDD history is associated with rumination. *Dev. Cogn. Neurosci.* 18, 89–100. doi: 10.1016/j.dcn.2015.11.003

Nemes-Baran, A. D., White, D. R., and DeSilva, T. M. (2020). Fractalkine-dependent microglial pruning of viable oligodendrocyte progenitor cells regulates myelination. *Cell Rep.* 32:108047. doi: 10.1016/j.celrep.2020.108047

Nesbitt, C., Van Der Walt, A., Butzkueven, H., Cheung, A. S., and Jokubaitis, V. G. (2025). Exploring the role of sex hormones and gender diversity in multiple sclerosis. *Nat. Rev. Neurol.* 21, 48–62. doi: 10.1038/s41582-024-01042-x

Nicholas, R. S. T. J., Wing, M. G., and Compston, A. (2001). Nonactivated microglia promote oligodendrocyte precursor survival and maturation through the transcription factor NF-κB. *Eur. J. Neurosci.* 13, 959–967. doi: 10.1046/j.0953-816X.2001.01470.x

Orso, R., Creutzberg, K. C., Lumertz, F. S., Kestering-Ferreira, E., Stocchero, B. A., Perrone, M. K., et al. (2023). A systematic review and multilevel meta-analysis of the prenatal and early life stress effects on rodent microglia, astrocyte, and oligodendrocyte density and morphology. *Neurosci. Biobehav. Rev.* 150:105202. doi: 10.1016/j.neubiorev.2023.105202

Pan, S., Mayoral, S. R., Choi, H. S., Chan, J. R., and Kheirbek, M. A. (2020). Preservation of a remote fear memory requires new myelin formation. *Nat. Neurosci.* 23, 487–499. doi: 10.1038/s41593-019-0582-1

Patani, R., Balaratnam, M., Vora, A., and Reynolds, R. (2007). Remyelination can be extensive in multiple sclerosis despite a long disease course. *Neuropathol. Appl. Neurobiol.* 33, 277–287. doi: 10.1111/j.1365-2990.2007.00805.x

Patel, R., Moore, S., Crawford, D. K., Hannsun, G., Sasidhar, M. V., Tan, K., et al. (2013). Attenuation of corpus callosum axon myelination and remyelination in the absence of circulating sex hormones. *Brain Pathol.* 23, 462–475. doi: 10.1111/bpa.12029

Pfeiffer, T., Avignone, E., and Nägerl, U. V. (2016). Induction of hippocampal long-term potentiation increases the morphological dynamics of microglial processes and prolongs their contacts with dendritic spines. *Sci. Rep.* 6:32422. doi: 10.1038/srep32422

Picard, K., Bisht, K., Poggini, S., Garofalo, S., Golia, M. T., Basilico, B., et al. (2021). Microglial-glucocorticoid receptor depletion alters the response of hippocampal microglia and neurons in a chronic unpredictable mild stress paradigm in female mice. *Brain Behav. Immun.* 97, 423–439. doi: 10.1016/j.bbi.2021.07.022

Poggi, G., Albiez, J., and Pryce, C. R. (2022). Effects of chronic social stress on oligodendrocyte proliferation-maturation and myelin status in prefrontal cortex and amygdala in adult mice. *Neurobiol. Stress* 18:100451. doi: 10.1016/j.ynstr.2022.100451

Poggi, G., Klaus, F., and Pryce, C. R. (2024). Pathophysiology in cortico-amygdala circuits and excessive aversion processing: the role of oligodendrocytes and myelination. *Brain Commun.* 6:fcae140. doi: 10.1093/braincomms/fcae140

Poggi, G., Portalés, A., Robert, M., Hofer, C., Schmid, S., Kúkeľová, D., et al. (2025). Chronic social stress induces generalized hyper-sensitivity to aversion: a mouse model with translational validity for understanding and treating negative valence disorders. *Neuropharmacology* 273:110430. doi: 10.1016/j.neuropharm.2025.110430

Rivers, L. E., Young, K. M., Rizzi, M., Jamen, F., Psachoulia, K., Wade, A., et al. (2008). PDGFRA/NG2 glia generate myelinating oligodendrocytes and piriform projection neurons in adult mice. *Nat. Neurosci.* 11, 1392–1401. doi: 10.1038/nn.2220

Santos, E. N., and Fields, R. Douglas. (2021). Regulation of Myelination by Microglia. Sci Adv. 7:eabk1131. doi: 10.1126/sciadv.abk1131

Sherafat, A., Pfeiffer, F., Reiss, A. M., Wood, W. M., and Nishiyama, A. (2021). Microglial neuropilin-1 promotes oligodendrocyte expansion during development and remyelination by trans-activating platelet-derived growth factor receptor. *Nat. Commun.* 12:2265. doi: 10.1038/s41467-021-22532-2

Sigrist, H., Hogg, D. E., Senn, A., and Pryce, C. R. (2024). Mouse model of chronic social stress-induced excessive Pavlovian aversion learning-memory. *Curr. Protoc.* 4:e1008. doi: 10.1002/cpz1.1008

Smith, K. L., Kassem, M. S., Clarke, D. J., Kuligowski, M. P., Bedoya-Pérez, M. A., Todd, S. M., et al. (2019). Microglial cell hyper-ramification and neuronal dendritic spine loss in the hippocampus and medial prefrontal cortex in a mouse model of PTSD. *Brain Behav. Immun.* 80, 889–899. doi: 10.1016/j.bbi.2019.05.042

Socodato, R., Henriques, J. F., Portugal, C. C., Almeida, T. O., Tedim-Moreira, J., Alves, R. L., et al. (2020). Daily alcohol intake triggers aberrant synaptic pruning leading to synapse loss and anxiety-like behavior. *Sci. Signal.* 13:eaba5754. doi: 10.1126/scisignal.aba5754

Süß, P., Hoffmann, A., Rothe, T., Ouyang, Z., Baum, W., Staszewski, O., et al. (2020). Chronic peripheral inflammation causes a region-specific myeloid response in the central nervous system. *Cell Rep.* 30, 4082–4095.e6. doi: 10.1016/j.celrep.2020.02.109

Taylor, D. L., Pirianov, G., Holland, S., McGinnity, C. J., Norman, A. L., Reali, C., et al. (2010). Attenuation of proliferation in oligodendrocyte precursor cells by activated microglia. *J. Neurosci. Res.* 88, 1632–1644. doi: 10.1002/jnr.22335

Wagner, J., Hoyer, C., Antony, H., Lundgrén, K., Soliymani, R., Crux, S., et al. (2026). Modulates Migration of Resident Microglia Towards Cortical Laser-Induced Lesions. Glia. 74:e70207. doi: 10.1002/glia.70207

Wallace, D. L., Han, M.-H., Graham, D. L., Green, T. a., Vialou, V., Iñiguez, S. D., et al. (2009). CREB regulation of nucleus accumbens excitability mediates social isolation-induced behavioral deficits. *Nat. Neurosci.* 12, 200–209. doi: 10.1038/nn.2257

Wicki, S., Canziani, A., Poggi, G., Argunşah, A. Ö., Karayannis, T., and Pryce, C. R. (2026). Development of visual-stimulus reversal learning-memory in mice is dependent on social interaction. *iScience* 29:114864. doi: 10.1016/j.isci.2026.114864

Wolswijk, G. (2002). Oligodendrocyte precursor cells in the demyelinated multiple sclerosis spinal cord. *Brain* 125, 338–349. doi: 10.1093/brain/awf031

Wood, S. K., and Bhatnagar, S. (2015). Resilience to the effects of social stress: evidence from clinical and preclinical studies on the role of coping strategies. *Neurobiol. Stress* 1, 164–173. doi: 10.1016/j.ynstr.2014.11.002

Xiong, J., Hagenauer, M. H., Rhoads, C. A., Flandreau, E., Rempel-Clower, N., Hernandez, E., et al. (2026). A Meta-analysis of the effects of chronic stress on the prefrontal transcriptome in animal models and convergence with existing human data. *Brain Behav.* 16:e71197. doi: 10.1002/brb3.71197

Xiong, Y., Hong, H., Liu, C., and Zhang, Y. Q. (2022). Social isolation and the brain: effects and mechanisms. *Mol. Psychiatry* 28, 191–201. doi: 10.1038/s41380-022-01835-w

Zhan, Y., Paolicelli, R. C., Sforazzini, F., Weinhard, L., Bolasco, G., Pagani, F., et al. (2014). Deficient neuron-microglia signaling results in impaired functional brain connectivity and social behavior. *Nat. Neurosci.* 17, 400–406. doi: 10.1038/nn.3641

Zhang, Y., Feng, W., Wang, Z., Pang, Y., Jin, Y., Chen, S., et al. (2023). Early growth response 2 in the mPFC regulates mouse social and cooperative behaviors. *Lab Anim. (NY).* 52, 37–50. doi: 10.1038/s41684-022-01090-0

Zhang, Y., Pang, Y., Feng, W., Jin, Y., Chen, S., Ding, S., et al. (2022). miR-124 regulates early isolation-induced social abnormalities via inhibiting myelinogenesis in the medial prefrontal cortex. *Cell. Mol. Life Sci.* 79, 507–524. doi: 10.1007/s00018-022-04533-6